PHYSICAL REVIEW B **79**, 060504(R) (2009)

Magnetic order in the $CaFe_{1-x}Co_xAsF$ ($x=0.00, 0.06, 0.12$) superconducting compounds

Y. Xiao,[1,*] Y. Su,[2] R. Mittal,[2,3] T. Chatterji,[4] T. Hansen,[5] C. M. N. Kumar,[1] S. Matsuishi,[6] H. Hosono,[6] and Th. Brueckel[1,2,4]

[1]*Institut fuer Festkoerperforschung, Forschungszentrum Juelich, D-52425 Juelich, Germany*

[2]*Juelich Centre for Neutron Science, IFF, Forschungszentrum Juelich, Outstation at FRM II, Lichtenbergstrasse 1, D-85747 Garching, Germany*

[3]*Solid State Physics Division, Bhabha Atomic Research Centre, Trombay, Mumbai 400085, India*

[4]*Juelich Centre for Neutron Science, Forschungszentrum Juelich, Outstation at Institut Laue-Langevin, BP 156, 38042 Grenoble Cedex 9, France*

[5]*Institut Laue-Langevin, BP 156, 38042 Grenoble Cedex 9, France*

[6]*Frontier Research Center, Tokyo Institute of Technology, 4259 Nagatsuta-cho, Midori-ku, Yokohama 226-8503, Japan*

(Received 27 November 2008; published 9 February 2009)

A neutron powder-diffraction experiment has been performed to investigate the structural phase transition and magnetic order in $CaFe_{1-x}Co_xAsF$ superconductor compounds ($x=0.00, 0.06, 0.12$). The parent compound CaFeAsF undergoes a tetragonal to orthorhombic phase transition at 134(3) K, while the magnetic order in the form of a spin-density wave (SDW) sets in at 114(3) K. The antiferromagnetic structure of the parent compound has been determined with a unique propagation vector $k=(1,0,1)$ and the Fe saturation moment of $0.49(5)\mu_B$, aligned along the long a axis. With increasing Co doping, the long-range antiferromagnetic order has been observed to coexist with superconductivity in the orthorhombic phase of the underdoped $CaFe_{0.94}Co_{0.06}AsF$ with a reduced Fe moment [$\sim 0.15(5)\mu_B$]. Magnetic order is completely suppressed in optimally doped $CaFe_{0.88}Co_{0.12}AsF$. We argue that the coexistence of SDW and superconductivity might be related to mesoscopic phase separation.

DOI: 10.1103/PhysRevB.79.060504 PACS number(s): 74.10.+v, 74.70.Dd, 75.25.+z, 75.50.Ee

The recent discovery of superconductivity in the iron-arsenic-based system $RFeAsO_{1-x}F_x$ (with R=La, Ce, Pr, etc.) has attracted tremendous amount of attention in the quest to understand the mechanism of high transition temperature superconductivity.[1–3] The superconducting transition temperature T_c has been quickly raised to 55 K via electron and hole dopings.[4–6] The second family of the FeAs-based superconductor system was discovered in $A_{1-x}B_xFe_2As_2$ (A=Ba, Sr, Ca, etc., and B=K or Na) with T_c up to 38 K.[7,8] Similar to the low dimensionality of high-T_c cuprate superconductors, both above-mentioned FeAs-based compounds adopt the layered structure with a single FeAs layer per unit cell of RFeAsO and two such layers per unit cell of AFe_2As_2. It is believed that the FeAs layers are responsible for the superconductivity because the electronic states near the Fermi surface are dominated by the contributions from Fe and As.[9,10]

Furthermore, these two iron-arsenic systems share another common feature: with decreasing temperature, their parent compounds undergo a structural distortion followed by the antiferromagnetic (AFM) order of Fe spins as revealed by latest neutron diffraction experiments on several parent compounds [LaFeAsO,[11] NdFeAsO,[12] $SrFe_2As_2$,[13] and $BaFe_2As_2$ (Ref. 14)]. The antiferromagnetic order in the parent compounds of iron pnictides is likely due to the spin-density wave (SDW) instability of a nested Fermi surface.[15,16] It has been observed in the neutron powder-diffraction (NPD) experiments that the iron moment is quite small [from $0.25\mu_B$ to $0.87\mu_B$ (Refs. 11–14)]. The origin of that small iron moment in these compounds was explained theoretically as the result of the itinerant character of iron spins[16] or the nearest-neighbor and next-nearest-neighbor superexchange interactions between Fe ions which give rise to a frustrated magnetic ground state.[17] Similar to the case in high-T_c cuprates, superconductivity in iron pnictides emerges upon electron or hole dopings, while static magnetic order is suppressed in the superconducting regime.[18,19] The role of possible spin fluctuations in promoting superconductivity in iron pnictides is still not clear yet.

Besides RFeAsO and AFe_2As_2, another FeAs-based superconductor system AFeAsF (with A=Ca, Sr, and Eu) was discovered very recently.[20–24] The parent compound AFeAsF crystallizes in the tetragonal ZrCuSiAs-type structure, where the $(RO)^+$ layers in RFeAsO are replaced by $(AF)^+$ layers. The local density approximation calculation indicated that both CaFeAsF and SrFeAsF have the same band dispersions in the vicinity of the Fermi level as the LaFeAsO compound.[25] For CaFeAsF, the optimal Co and Ni doping on the Fe site induces the superconducting phase with T_c=22 and 12 K, respectively.[26] The higher superconducting transition temperature can be reached by doping rare-earth ions into the Ca site, e.g., T_c=52.8 K for $Ca_{0.4}Pr_{0.6}FeAsF$ and T_c=57.4 K for $Ca_{0.4}Nd_{0.6}FeAsF$.[27] The T_c of $Ca_{0.4}Nd_{0.6}FeAsF$ is so far the highest T_c observed in the FeAs-based superconductors. Considering that the AFeAsF forms the same structure as LaFeAsO, the parent compound of the first FeAs-based superconductor system, it is interesting to investigate the phase diagram of that oxygen-free system and compare it with the LaFeAsO system.

In the present work, we report the neutron powder-diffraction experiment on the $CaFe_{1-x}Co_xAsF$ ($x=0.00, 0.06, 0.12$) superconductor compounds. The magnetic and crystal structures of the CaFeAsF parent compound have been determined via the Rietveld refinement. The evolution of magnetic order and crystal structure in the Co-doped $CaFe_{0.94}Co_{0.06}AsF$ and $CaFe_{0.88}Co_{0.12}AsF$ are also presented. Furthermore, both NPD and detailed characterizations of the superconducting property in the slightly underdoped $CaFe_{0.94}Co_{0.06}AsF$ compound suggest that SDW and

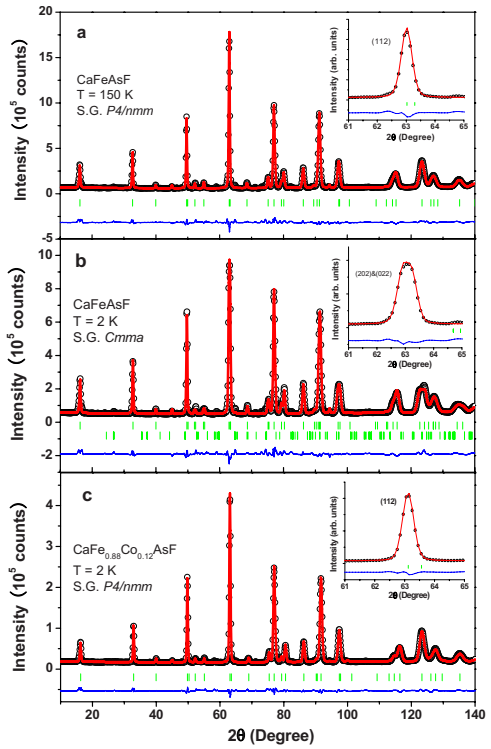

FIG. 1. (Color online) NPD refinement patterns for CaFeAsF at (a) 150 and (b) 2 K and for $CaFe_{0.88}Co_{0.12}AsF$ at (c) 2 K. The circles represent the observed intensity; the solid line is the calculated pattern. The difference between the observed and calculated intensities is shown at the bottom. The vertical bars indicate the expected Bragg reflection positions. The insets of (a), (b), and (c) show the $(112)_T$ reflection of tetragonal phase and the splitting of $(112)_T$ reflection in orthorhombic phase, respectively.

superconductivity may coexist on the mesoscopic scale. The polycrystalline samples of 10 g each were synthesized by a solid-state reaction method as described in Ref. 20 with impurity phases (CaF_2 and Fe_2O_3) of less than 1%. The neutron powder-diffraction measurements were performed on the high flux powder diffractometer D20 at Institut Laue-Langevin (Grenoble, France). A pyrolitic graphite (PG) (002) monochromator was used to produce a monochromatic neutron beam of wavelength 2.42 Å. The sample was loaded in a vanadium sample holder and then installed in the liquid helium cryostat. The program FULLPROF (Ref. 28) was used for the Rietveld refinement of the crystal and the magnetic structures of the compounds.

The CaFeAsF crystallizes in the tetragonal structure with space group $P4/nmm$ at 150 K as shown in Fig. 1(a). With decreasing temperature the CaFeAsF undergoes an orthorhombic distortion (space group *Cmma*) as revealed by the NPD pattern measured at 2 K [Fig. 1(b)]. The splitting of the $(112)_T$ reflection [insets of Figs. 1(a) and 1(b)] could not be resolved due to the limited resolution and the small difference in lattice parameters a and b. However, the splitting is obvious from the observed peak broadening. In order to clarify the structural transition, the peak intensity and full width at half maximum (FWHM) of the $(112)_T$ reflection are plotted in Fig. 2(a). The sharp decrease in the intensity and the significant broadening of FWHM reveal the occurrence

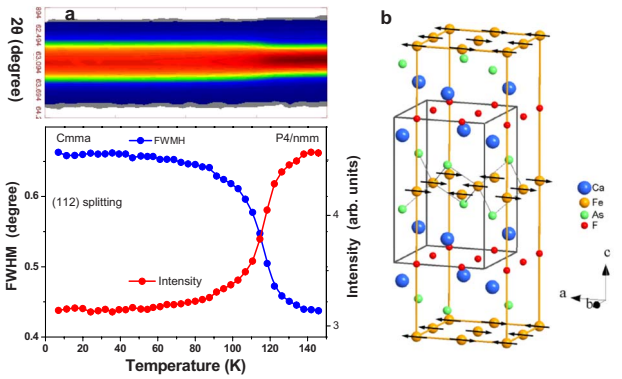

FIG. 2. (Color online) (a) Temperature dependence of the peak intensity and the FWHM of $(112)_T$ peak in CaFeAsF. The decrease in intensity and increase in the FWHM reveals occurrence of the orthorhombic distortion. (b) Illustration of the magnetic structures of CaFeAsF below the magnetic transition temperature. The Fe moments align along a direction and ordered antiferromagnetically in both a and c directions. The magnetic unit cell doubles along the c axis as shown in the orange (light gray) bonds while the gray line outlines the tetragonal unit cell.

of the tetragonal to orthorhombic structural transition. From the onset of the broadening of the $(112)_T$ reflection, we estimate the phase-transition temperature to be in the range of 131–137 K.

Compared with the NPD pattern at 150 K, the magnetic reflections appear at lower temperature for CaFeAsF. The temperature evolution of the magnetic reflection between 33.6° and 37.4° is shown in Fig. 3(a), which indicates the appearance of long-range magnetic order. The integrated in-

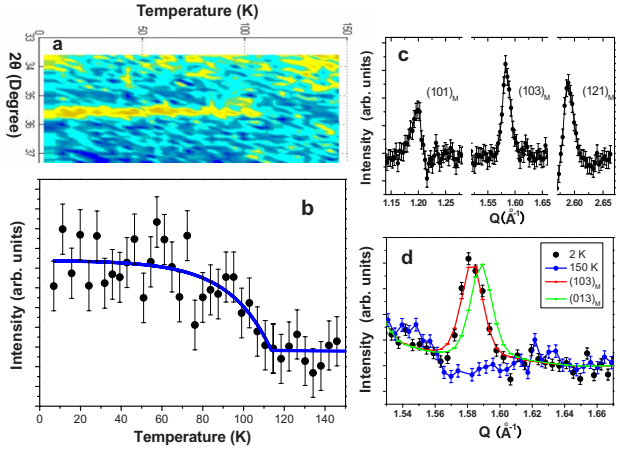

FIG. 3. (Color online) (a) Temperature evolution of the reflection at $Q=1.583$ $Å^{-1}$ indicating the onset of long-range magnetic ordering in CaFeAsF. (b) Temperature dependence of the integrated intensity of magnetic Bragg reflection. (c) The magnetic reflections obtained by subtracting the NPD pattern measured at 150 K from the pattern measured at 2 K. The asymmetric peak shape is due to neighboring reflections. (d) Comparison of NPD patterns for CaFeAsF measured at 2 K (black) and 150 K (blue), respectively. The red and green curves are the calculated patterns of $(103)_M$ and $(013)_M$ reflections, respectively. The magnetic peak at $Q=1.583$ $Å^{-1}$ can be indexed as the $(103)_M$ properly within the magnetic unit cell.

TABLE I. The observed intensity of magnetic reflections and the calculated value for different magnetic models.

Reflection	I_{Obs}	$I_{Calc.}[(1,0,1), a]^a$	$I_{Calc.}[(0,1,1), a]^a$
$(101)_M/(011)_M$	396(93)	301	3173
$(103)_M/(013)_M$	830(87)	825	1697
$(121)_M/(211)_M$	739(88)	766	210

[a]The propagation vector and the moment direction are shown in brackets.

tensity of the magnetic reflection at $Q=1.583$ Å^{-1} is plotted in Fig. 3(b). The solid curve is a power law fit to estimate a Néel temperature of 114(3) K. A series of magnetic peaks can be noticed clearly as shown in Fig. 3(c) by subtracting the NPD pattern measured at 150 K from the pattern measured at 2 K. By indexing the magnetic Bragg peaks, we find that the magnetic ordering of CaFeAsF at 2 K can be described within an antiferromagnetic model where the magnetic unit cell is doubled along the c axis. The Fe moments are coupled antiferromagneticlly along the c direction, while in the ab plane, the Fe moment are ordered antiferromagnetically along one axis and ferromagnetically along another axis. This antiferromagnetic model is exactly the same as the magnetic structure found by neutron powder diffraction for LaFeAsO (Ref. 11) and NdFeAsO.[12] However, for both LaFeAsO and NdFeAsO the precise Fe moment direction in the ab plane of the orthorhombic structure could not be determined due to the weak magnetic intensity and small difference of the respective magnetic peak positions corresponding to the Fe moment aligned along the a or b direction. In the present work, the high intensity diffraction data that we collected from D20 allows us to determine the exact propagation vector and the iron moment direction within the ab plane. For those configurations in which k is perpendicular to the moment direction, i.e., $k=(1,0,1)$ with the Fe moment along the b direction or $k=(0,1,1)$ with the Fe moment along the a direction, the intensity ratio between (101)/(011), (103)/(013), and (121)/(211) was expected to be 32:17:2 due to the difference of the Fe magnetic form factor in the corresponding Q position (Table I). However, based on our NPD results, the intensity of the (121)/(211) reflection is observed to be stronger than the (101)/(011) reflection [Fig. 3(c) and Table I]. Therefore, these configurations can be ruled out. As shown in Fig. 3(d), the reflection at $Q=1.583$ Å^{-1} can be fitted properly as the (103) magnetic reflection with the moment along the a direction, whereas the position of the (013) reflection is slightly shifted to a higher Q position at $Q=1.589$ Å^{-1}. Therefore, the magnetic structure of CaFeAsF can be unambiguously determined as an antiferromagnetic structure with Fe moment along the long a axis in the orthorhombic unit cell as shown in Fig. 2(b). The Fe moment derived from NPD results is $0.49(5)\mu_B$, which is considerably larger than the moment observed in LaFeAsO ($0.35\mu_B$) and NdFeAsO ($0.25\mu_B$) but smaller than the moment observed in $BaFe_2As_2$ ($0.8\mu_B$) and $SrFe_2As_2$ ($0.94\mu_B$). Note that the origin of the observed large difference of the Fe moment in iron pnictides is still not clear, while the same antiferromagnetic structure due to SDW instabilities of a nested Fermi surface have been observed among all compounds.

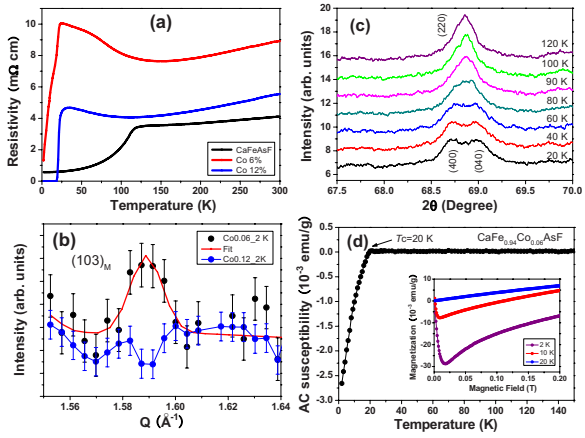

FIG. 4. (Color online) Temperature dependence of electrical resistivity of $Ca(Fe_{1-x}Co_x)AsF$, with $x=0.00$, 0.06, and 0.12. (b) The magnetic reflection still exists for $CaFe_{0.94}Co_{0.06}AsF$ (black) at 2 K and it is not observed for $CaFe_{0.88}Co_{0.12}AsF$ (blue) at 2 K. (c) The splitting of (220) reflection with increasing temperature for $CaFe_{0.94}Co_{0.06}AsF$. (d) Temperature dependence of the real component of the ac susceptibility and the magnetization (inset) for $CaFe_{0.94}Co_{0.06}AsF$.

Both the structural and magnetic phase transitions have thus been determined for parent compound CaFeAsF. Recently, Zhao *et al.*[18] found that the highest T_c of FeAs-based compounds can be obtained when the Fe-As-Fe bond angle is close to the ideal value of 109.47°, as expected from a perfect FeAs tetrahedron. The effective way to increase T_c in FeAs-based systems is to optimize the Fe-As-Fe angle. It can be noticed that the Fe-As-Fe bond angle in CaFeAsF is 108.55° which is relatively close to the ideal value compared with LaFeAsO and $BaFe_2As_2$. Therefore the CaFeAsF is suggested to be a promising system for maximizing T_c. In addition, it should be emphasized that the two phase transitions in CaFeAsF occur at different temperatures, 134(3) K for structural and 114(3) K for magnetic phase transitions. Separated phase transitions are also observed in LaFeAsO (Ref. 11) and CeFeAsO.[18] However, for the LaFeAsO, the anomaly in resistivity is associated with the structural transition; but according to the resistivity measurement on CaFeAsF [Fig. 4(a)], the anomaly in resistivity takes place at around 120 K which is closer to the magnetic phase transition. Therefore, the decrease in resistivity is likely associated with the SDW transition in CaFeAsF.

In order to investigate in detail the change in the crystal structure and the variation in SDW across the superconducting boundary, the NPD measurement was also carried out on the $Ca(Fe_{1-x}Co_x)AsF$, with $x=0.06$ and 0.12. For the superconductor $Ca(Fe_{0.88}Co_{0.12})AsF$, the tetragonal structure persists down to 2 K, and no evidence of SDW is observed [Fig. 1(c)]. This would indicate that the SDW in the $Ca(Fe_{1-x}Co_x)AsF$ system is totally suppressed in the superconducting state with an optimal Co doping level. For the slightly underdoped $Ca(Fe_{0.94}Co_{0.06})AsF$ compound, the SDW survives at 2 K as shown in Fig. 4(b) and the Fe moment is reduced to $0.15(5)\mu_B$. To determine the structural

phase transition of $Ca(Fe_{0.94}Co_{0.06})AsF$, a conventional laboratory x-ray diffractometer was used to collect x-ray powder-diffraction patterns under different temperatures as shown in Fig. 4(c). Based on the splitting of the $(220)_T$ reflection, the tetragonal to orthorhombic phase-transition temperature is determined to be around 85(3) K, which is lower than that of parent compound CaFeAsF. The orthorhombic distortion parameter $P=(a-b)/(a+b)$ is deduced to be 0.17% for the 6% Co-doped compound at 2 K, while it is 0.34% for the parent compound. It seems that there exists a close relation between the order parameter P and the Fe moment value; in other words, the smaller orthorhombic splitting will lead to a weaker SDW ordering. Figure 4(d) shows the temperature dependence of ac susceptibility of $Ca(Fe_{0.94}Co_{0.06})AsF$; the strong diamagnetic signal exhibits below 20 K, which corresponds to the anomaly observed in the resistivity-temperature curve. The temperature dependence of magnetization also supports the existence of the Meissner state as shown in the inset of Fig. 4(d). Therefore, the coexistence of SDW and superconductivity can be confirmed in $Ca(Fe_{0.94}Co_{0.06})AsF$. Moreover, the superconductivity can occur either in the tetragonal (with $x=0.12$) or orthorhombic (with $x=0.06$) structure in the $Ca(Fe_{1-x}Co_x)AsF$ system. Presently, several phase diagrams have been constructed for different FeAs-based superconductor systems. However, the different systems always exhibit different behaviors around the phase boundary between the antiferromagnetic and superconducting regimes. For example, there is no overlap between those two phases in the LaFeAsOF (Ref. 29) and the CeFeAsOF (Ref. 18) systems, while a slightly overlap was observed in the SmFeAsFO (Refs. 30 and 31) system and the broad overlap composition range in the $Ba_{1-x}K_xFeAs$ system.[19,32] Although the mechanism of such coexistence is still not clear, the phase separation on the macroscopic scale can be ruled out since the single orthorhombic phase was clearly revealed by synchrotron x-ray for $Ba_{1-x}K_xFeAs$ (Ref. 19) and by laboratory x-ray for our $Ca(Fe_{0.94}Co_{0.06})AsF$ case. Recently, mesoscopic phase separation was suggested by Park *et al.*[33] in underdoped $Ba_{1-x}K_xFeAs$ superconductors. Very recent μSR experiments also indicate the presence of mesoscopic phase separation into superconducting and magnetic phases in the $Ca(Fe_{1-x}Co_x)AsF$ system across the phase boundaries.[34] Therefore, such mesoscopic phase separation might be considered as an intrinsic property, and it may explain the coexistence of antiferromagnetic and superconducting states in some FeAs-based superconducting systems.

In summary, by using high flux neutron powder diffraction we have observed the tetragonal to orthorhombic structural transition at 134(3) K followed by the magnetic structure transition at 114(3) K in CaFeAsFe. Below T_N, long-range antiferromagnetic ordering with a propagation vector $k=(1,0,1)$ and an Fe moment of $0.49(5)\mu_B$ and of $0.15(5)\mu_B$ for parent and 6% Co-doped compounds, respectively. With increasing Co doping on the Fe site the SDW is weakened in the 6% Co-doped compound and completely suppressed in the 12% Co-doped compound. The observed coexistence of antiferromagnetic and superconducting states might be explained as due to the mesoscopic phase separation.

*y.xiao@fz-juelich.de

[1] Y. Kamihara *et al.*, J. Am. Chem. Soc. **130**, 3296 (2008).
[2] H. Takahashi *et al.*, Nature (London) **453**, 376 (2008).
[3] X. H. Chen *et al.*, Nature (London) **453**, 761 (2008).
[4] Z.-A. Ren *et al.*, Chin. Phys. Lett. **25**, 2215 (2008).
[5] C. Wang *et al.*, EPL **83**, 67006 (2008).
[6] H. H. Wen *et al.*, EPL **82**, 17009 (2008).
[7] M. Rotter *et al.*, Phys. Rev. Lett. **101**, 107006 (2008).
[8] A. I. Goldman *et al.*, Phys. Rev. B **78**, 100506(R) 2008.
[9] D. J. Singh and M.-H. Du, Phys. Rev. Lett. **100**, 237003 (2008).
[10] K. Haule *et al.*, Phys. Rev. Lett. **100**, 226402 (2008).
[11] C. de la Cruz *et al.*, Nature (London) **453**, 899 (2008).
[12] Y. Chen *et al.*, Phys. Rev. B **78**, 064515 (2008).
[13] J. Zhao *et al.*, Phys. Rev. B **78**, 140504(R) (2008).
[14] Y. Su *et al.*, arXiv:0807.1743 (unpublished).
[15] Z. P. Yin *et al.*, Phys. Rev. Lett. **101**, 047001 (2008).
[16] I. I. Mazin *et al.*, Phys. Rev. Lett. **101**, 057003 (2008).
[17] T. Yildirim, Phys. Rev. Lett. **101**, 057010 (2008).
[18] J. Zhao *et al.*, Nature Mater. **7**, 953 (2008).
[19] H. Chen *et al.*, EPL **85**, 17006 (2009).
[20] S. Matsuishi *et al.*, J. Am. Chem. Soc. **130**, 14428 (2008).
[21] F. Han *et al.*, Phys. Rev. B **78**, 180503(R) (2008).
[22] M. Tegel *et al.*, EPL **84**, 67007 (2008).
[23] X. Zhu *et al.*, EPL **85**, 17011 (2009).
[24] S. Matsuishi *et al.*, J. Phys. Soc. Jpn. **77**, 113709 (2008).
[25] I. A. Nekrasov *et al.*, JETP Lett. **88**, 543 (2008).
[26] S. Matsuishi *et al.*, arXiv:0811.1147 (unpublished).
[27] P. Cheng *et al.*, arXiv:0812.1192 (unpublished).
[28] J. Rodríguez-Carvajal, Physica B **192**, 55 (1993).
[29] H. Luetkens *et al.*, arXiv:0806.3533 (unpublished).
[30] A. J. Drew *et al.*, Phys. Rev. Lett. **101**, 097010 (2008).
[31] R. H. Liu *et al.*, Phys. Rev. Lett. **101**, 087001 (2008).
[32] T. Goko *et al.*, arXiv:0808.1425 (unpublished).
[33] J. T. Park *et al.*, arXiv:0811.2224 (unpublished).
[34] S. Takeshita *et al.*, arXiv:0812.1670 (unpublished).